Available online at www.sciencedirect.com
SCIENCE DIRECT®
Journal of Nuclear Materials 336 (2005) 177–184
journal of nuclear materials
www.elsevier.com/locate/jnucmat

# Thermodynamic stabilities of $SrCeO_3$ and $Sr_2CeO_4$ using the fluoride EMF technique

R. Pankajavalli, K. Ananthasivan, S. Anthonysamy, P.R. Vasudeva Rao *

*Fuel Chemistry Division, Chemical Group, Indira Gandhi Centre for Atomic Research, Kalpakkam 603 102, India*

Received 3 June 2004; accepted 17 September 2004

**Abstract**

The standard Gibbs energies of formation of $SrCeO_3$ and $Sr_2CeO_4$ were measured by the EMF method using $CaF_2$ as a solid electrolyte. Three fluoride galvanic cells (I–III) were constructed in order to determine $\Delta_f G^\circ$ of $SrCeO_3$. The $\Delta_f G^\circ$ of $Sr_2CeO_4$ was determined using galvanic cell (IV). The cells used were

$$\text{Pt, } O_2(g)\ (1\,\text{bar}),\ SrO(s),\ SrF_2(s)|CaF_2|SrF_2(s),\ CeO_2(s),\ SrCeO_3(s),\ O_2(g)\ (1\,\text{bar}),\ \text{Pt} \quad \text{(I)}$$

$$\text{Pt, } O_2(g)\ (1\,\text{bar}),\ SrO(s),\ SrF_2(s)|SrF_2|SrF_2(s),\ CeO_2(s),\ SrCeO_3(s),\ O_2(g)\ (1\,\text{bar}),\ \text{Pt} \quad \text{(II)}$$

$$\text{Pt, } O_2(g)\ (1\,\text{bar}),\ SrF_2(s),\ CeO_2(s),\ SrCeO_3(s)|CaF_2|CaF_2(s),\ CaO(s),\ O_2\ (1\,\text{bar}),\ \text{Pt} \quad \text{(III)}$$

$$\text{Pt, } O_2(g)\ (1\,\text{bar}),\ SrO(s),\ SrF_2(s)|CaF_2|SrF_2(s),\ SrCeO_3(s),\ Sr_2CeO_4(s),\ O_2\ (1\,\text{bar}),\ \text{Pt} \quad \text{(IV)}$$

The standard Gibbs energy of formation of $SrCeO_3$, derived from the mean of the EMFs of the above galvanic cells (I to III), is given by the following expression:

$$\Delta_f G^\circ(SrCeO_3) \pm 17\ (\text{kJ mol}^{-1}) = -1703 + 0.327T\ (\text{K})\ (788\text{–}1142\,\text{K})$$

By combining this expression with the EMF measured using Cell IV, the following expression was obtained for the temperature dependence of the standard Gibbs energy of formation of $Sr_2CeO_4$

$$\Delta_f G^\circ(Sr_2CeO_4) \pm 21(\text{kJ mol}^{-1}) = -2307 + 0.4400\,T\ (\text{K})(805\text{–}1066\,\text{K})$$



* Corresponding author. Tel.: +91 4114 280229/40229; fax: +91 4114 280065.
*E-mail address:* vasu@igcar.ernet.in (P.R. Vasudeva Rao).

0022-3115/$ - see front matter © 2004 Elsevier B.V. All rights reserved.
doi:10.1016/j.jnucmat.2004.09.012

## 1. Introduction

The Prototype Fast Breeder Reactor (PFBR) in India would use a mixed oxide of uranium and plutonium (MOX, containing $PuO_2$ fractions of 0.21 and 0.28) as fuel [1,2]. The complex chemical equilibria existing in the fuel during reactor operation have been studied in great detail in the past [3]. However, further investigations are required in order to augment the existing data. These would be useful for understanding the complex chemistry of the MOX fuel during its life in the reactor. Ceria is often considered to be an inactive substitute for plutonia [4]. Thus, a study of the ternary oxides bearing cerium could serve as a forerunner for the experiments on plutonium bearing fuel materials. Hence an experimental programme is underway at our Centre for the determination of stabilities of various ceramic oxides bearing plutonium. In this study the stabilities of two ternary oxides of cerium with strontium were examined.

There are two ternary oxides namely $SrCeO_3$ and $Sr_2CeO_4$ reported in the literature in the pseudo-binary system SrO–$CeO_2$ [5]. A tentative partial isothermal section of the system Sr–Ce–O, at 1073 K is given in Fig. 1. Saha et al. [6] reported the enthalpy increment measurements of $SrCeO_3$ using a high-temperature drop calorimetry technique. Gopalan and Virkar [7] measured the thermodynamic stability of $SrCeO_3$ through EMF measurements by constructing galvanic cells with a molten salt electrolyte as well as $CaF_2$ solid electrolyte. Cordfunke et al. [8] reported data on the heat capacity and standard molar enthalpy of formation ($\Delta_f H^\circ_{298}$) of $SrCeO_3$ using solution calorimetry. Yamanaka et al. [9] have determined the heat capacity and thermal expansion of $SrCeO_3$ using differential scanning calorimetry and dilatometry respectively. Ali et al. [10] determined the standard molar enthalpy of formation of $Sr_2CeO_4$ using an isoperibol calorimeter. Although several thermal properties have been studied, no experimental investigations have been carried out to measure the standard Gibbs energy of formation of these ternary compounds. The thermodynamic characterization of the system Sr–Ce–O using yttria stabilized zirconia or yttria doped thoria electrolytes would be difficult owing to the extremely low oxygen potentials involved. However, fluoride electrolytes can be successfully employed to measure the low oxygen potentials in the system Sr–Ce–O. Hence, the present study was undertaken with a view to determine $\Delta_f G^\circ$ of $SrCeO_3$ and $Sr_2CeO_4$ using the fluoride EMF technique.

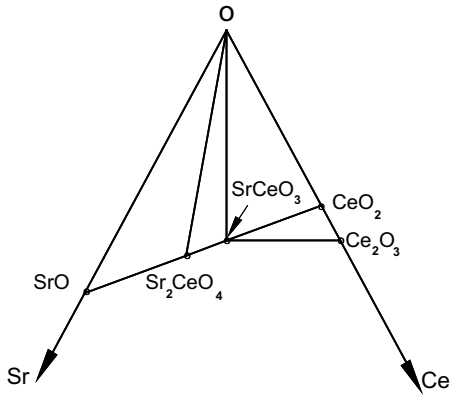


Fig. 1. Partial isothermal section of the Sr–Ce–O phase diagram at 1073 K.

## 2. Experimental

### 2.1. Materials

Nuclear grade cerium (III) nitrate hexahydrate, $CeO_2$ (purity > 99.99%, Indian Rare Earths Ltd., Mumbai) and strontium nitrate (purity > 99.9%, Fluka Germany) were used. In addition, $SrCO_3$ and $CaCO_3$ (purity > 99.9%, IDPL, India) were used for the solid-state synthesis of SrO and CaO, respectively. Polycrystalline $SrF_2$ and $CaF_2$ (purity > 99.99%, Aldrich, USA) were used for making the $SrF_2$ electrolyte as well as for use as electrode materials. Other chemicals such as nitric acid (Reachem Laboratory Chemicals Pvt. Ltd., Chennai) and citric acid (Fischer Inorganics and Aromatics Ltd., Chennai) were of reagent grade.

### 2.2. Sample preparation

The ternary compounds $SrCeO_3$ and $Sr_2CeO_4$ were synthesized by the gel-combustion procedure [11]. In this method, a saturated aqueous solution containing desired amounts of strontium nitrate, cerium nitrate hexahydrate and citric acid was heated on a hot plate. This solution progressively thickened yielding a dry gel, which finally got ignited through a self-sustaining combustion reaction. The product obtained in this reaction was a yellow oxide powder. This product was calcined in air at 923 K for 4 h in order to remove the residual carbon present in it. The final product was compacted into cylindrical pellets of 10 mm diameter by applying a pressure of 100 MPa in a hydraulic press. These pellets were then sintered at 1373 K for 12 h in air. The phase composition of the ternary compounds synthesized as mentioned above was ascertained by powder X-ray diffraction (XRD) analysis (Philips X-ray diffractometer, The Netherlands) within the 5 mass percent limit of detection of the impurity phases using CuK$\alpha$ radiation. The XRD pattern pertaining to $SrCeO_3$ synthesized using the above method is given in Fig. 2. The XRD data of this perovskite phase corresponds to an orthorhombic unit cell with lattice parameters $b = 857.6(6)$

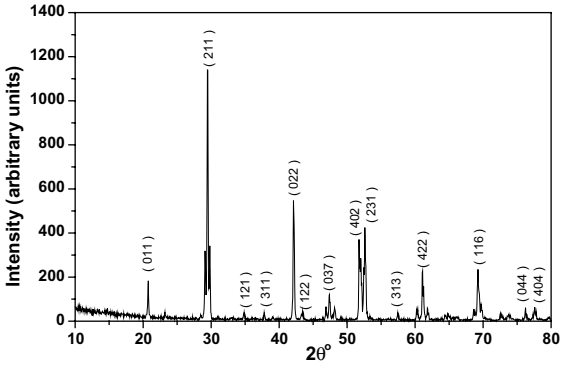


Fig. 2. XRD pattern of $SrCeO_3$.

pm, $a = 614.6(3)$ pm and $c = 600.8(4)$ pm and space group – Pnma (62). The XRD pattern of $Sr_2CeO_4$ showed the presence of traces of $SrCeO_3$. This phase mixture was used for the preparation of the test electrode, $Sr_2CeO_4/SrCeO_3/SrF_2$.

For the synthesis of polycrystalline $SrF_2$ electrolyte, well-dried $SrF_2$ powder was compacted into cylindrical pellets of 15 mm diameter and 3–4 mm thickness at a pressure of 300 MPa in a hydraulic press. These pellets were loaded in a zirconia boat and sintered at 1693 K for 2 h under controlled flow of the argon gas in a Pt wire wound furnace. A slow heating rate of 5 K $min^{-1}$ was employed in order to facilitate recrystallization. Subsequently, the temperature was reduced to 1523 K (cooling rate 3 K $min^{-1}$) and maintained at that temperature for 12 h in order to minimize vaporization and pore formation. The density of these pellets was measured by liquid immersion technique with dibutyl phthalate as the immersion liquid. The average density of these electrolyte discs was found to be 3.918 Mg $m^{-3}$ (≈93% theoretical density (TD)).

SrO and CaO were prepared by decomposition of $SrCO_3$ and $CaCO_3$ powders, respectively. The oxide powders were then compacted into cylindrical pellets and heated at 1473 K under flowing of purified oxygen for 5 h. The products thus obtained were cooled in a stream of high-purity helium down to a temperature of 1073 K and quenched in order to prevent the formation of the respective carbonates and higher oxides like $SrO_2$.

### 2.3. EMF measurements

An open cell-stacked pellet assembly as described elsewhere [12] was employed for the EMF measurement. In this study, single crystal $CaF_2$ and polycrystalline $SrF_2$ were used as the electrolytes for the direct measurement of high-temperature thermodynamic properties of compounds of a highly electropositive metal like cerium. Two separate three-phase mixtures, $SrCeO_3(s)/CeO_2(s)/SrF_2(s)$ and $Sr_2CeO_4(s)/SrCeO_3(s)/SrF_2(s)$ made into cylindrical pellets were used as test electrodes. Similarly, compacts of two separate two-phase mixtures $SrO(s)/SrF_2(s)$ and $CaO(s)/CaF_2(s)$ prepared without exposing them to air were used as the reference electrodes. Pure $O_2$ at 1 bar was used as the cover gas after passing through suitable drying agents. All temperature measurements were made using a pre-calibrated Type-S thermocouple whose hot junction was located in the proximity of the galvanic cell, which in turn was placed in the uniform temperature zone to minimize thermoelectric contributions. The attainment of equilibrium during the EMF measurements was verified not only by thermal cycling and micro-polarization but also by marginal variation in the ratio of the co-existing phases. All other experimental details are the same as described elsewhere [12,13]. The following galvanic cells were used and the EMF of these cells was measured as a function of temperature.

$$\text{Pt, } O_2(g)\ (1\,\text{bar}),\ SrO(s),\ SrF_2(s)|CaF_2|SrF_2(s),\ CeO_2(s),\ SrCeO_3(s),\ O_2(g)\ (1\,\text{bar}),\ \text{Pt} \quad \text{(I)}$$

$$\text{Pt, } O_2(g)\ (1\,\text{bar}),\ SrO(s),\ SrF_2(s)|SrF_2|SrF_2(s),\ CeO_2(s),\ SrCeO_3(s),\ O_2(g)\ (1\,\text{bar}),\ \text{Pt} \quad \text{(II)}$$

$$\text{Pt, } O_2(g)\ (1\,\text{bar}),\ SrF_2(s),\ CeO_2(s),\ SrCeO_3(s)|CaF_2|CaF_2(s),\ CaO(s),\ O_2\ (1\,\text{bar}),\ \text{Pt} \quad \text{(III)}$$

$$\text{Pt, } O_2(g)\ (1\,\text{bar}),\ SrO(s),\ SrF_2(s)|CaF_2|SrF_2(s),\ SrCeO_3(s),\ Sr_2CeO_4(s),\ O_2\ (1\,\text{bar}),\ \text{Pt} \quad \text{(IV)}$$

## 3. Results

The EMF data obtained using the cells (I)–(IV) are given in Tables 1–4. These results are represented by the following least-squares expressions. The ranges of temperatures over which these expressions are valid are indicated within parentheses.

$$(E_{\text{I}} \pm 1.0)\ (\text{mV}) = 126.72 - 0.11101T\ (\text{K}),\quad (837\text{–}976\,\text{K}) \quad (1)$$

$$(E_{\text{II}} \pm 0.8)\ (\text{mV}) = 79.34 - 0.06364T\ (\text{K}),\quad (788\text{–}954\,\text{K}) \quad (2)$$

Table 1
Temperature dependence of EMF of cell I

| Run | $T$ (K) | EMF (mV) | Run | $T$ (K) | EMF (mV) | Run | $T$ (K) | EMF (mV) |
|---|---|---|---|---|---|---|---|---|
| A1 | 872.9 | 28.8 | B1 | 882.9 | 27.4 | C1 | 836.5 | 32.9 |
| A2 | 890.9 | 27.5 | B2 | 896.2 | 28.9 | C2 | 858.0 | 32.0 |
| A3 | 907.0 | 26.7 | B3 | 896.7 | 26.8 | C3 | 874.5 | 31.1 |
| A4 | 913.2 | 25.5 | B4 | 911.7 | 26.5 | C4 | 884.2 | 27.4 |
| A5 | 923.2 | 24.9 | B5 | 928.5 | 23.4 | C5 | 891.4 | 28.6 |
| A6 | 940.0 | 22.6 | B6 | 930.0 | 24.2 | C6 | 907.2 | 24.9 |
| A7 | 946.5 | 22.2 | B7 | 946.2 | 22.1 | C7 | 909.7 | 25.8 |
| A8 | 956.2 | 20.7 | B8 | 947.0 | 23.3 | C8 | 931.7 | 23.5 |
| A9 | 968.5 | 19.4 | B9 | 961.5 | 18.9 | C9 | 958.2 | 17.7 |
| A10 | 973.2 | 17.9 | B10 | 963.5 | 18.8 | C10 | 975.7 | 19.5 |

Table 2
Temperature dependence of EMF of cell II

| Run | $T$ (K) | EMF (mV) | Run | $T$ (K) | EMF (mV) |
|---|---|---|---|---|---|
| A1 | 879.2 | 23.7 | B1 | 789.4 | 29.7 |
| A2 | 895.2 | 22.5 | B2 | 805.0 | 29.0 |
| A3 | 912.5 | 20.9 | B3 | 821.2 | 26.5 |
| A4 | 930.2 | 19.8 | B4 | 837.2 | 24.5 |
| A5 | 953.5 | 19.3 | B5 | 866.0 | 24.6 |

Table 3
Temperature dependence of EMF of cell III

| Run | $T$ (K) | EMF (mV) | Run | $T$ (K) | EMF (mV) |
|---|---|---|---|---|---|
| A1 | 1006.2 | 120.0 | B1 | 972.2 | 120.8 |
| A2 | 1023.0 | 119.7 | B2 | 1017.5 | 119.5 |
| A3 | 1040.2 | 118.3 | B3 | 1018.7 | 119.7 |
| A4 | 1050.2 | 118.8 | B4 | 1035.4 | 118.5 |
| A5 | 1057.0 | 118.2 | B5 | 1040.7 | 118.7 |
| A6 | 1068.0 | 118.5 | B6 | 1050.5 | 118.3 |
| A7 | 1075.0 | 117.3 | B7 | 1064.5 | 117.2 |
| A8 | 1086.0 | 117.8 | B8 | 1076.7 | 117.2 |
| A9 | 1093.2 | 116.4 | B9 | 1087.7 | 116.9 |
| A10 | 1103.0 | 116.6 | B10 | 1101.0 | 117.1 |
| A11 | 1110.2 | 116.8 | B11 | 1106.2 | 116.3 |
| A12 | 1120.7 | 116.1 | B12 | 1142.0 | 116.5 |

Table 4
Temperature dependence of EMF of cell IV

| Run | $T$ (K) | EMF (mV) | Run | $T$ (K) | EMF (mV) |
|---|---|---|---|---|---|
| A1 | 804.5 | 14.4 | B1 | 857.7 | 13.3 |
| A2 | 847.5 | 14.2 | B2 | 874.2 | 12.8 |
| A3 | 869.7 | 13.8 | B3 | 891.5 | 12.1 |
| A4 | 893.0 | 12.1 | B4 | 908.7 | 10.8 |
| A5 | 972.7 | 6.5 | B5 | 925.7 | 9.1 |
| A6 | 986.7 | 7.0 | B6 | 944.2 | 6.9 |
| A7 | 1018.7 | 3.0 | B7 | 1006.5 | 6.0 |
| A8 | 1042.5 | 1.5 | B8 | 1024.4 | 4.2 |
| A9 | 1066.0 | 2.1 | B9 | 1040.5 | 3.6 |
| | | | B10 | 1059.2 | 3.2 |

$$(E_{III} \pm 0.4)\ (\mathrm{mV}) = 150.65 - 0.0307T\ (\mathrm{K}),\quad (972\text{–}1142\,\mathrm{K}) \tag{3}$$

$$(E_{IV} \pm 1.0)\ (\mathrm{mV}) = 60.24 - 0.05478T\ (\mathrm{K}),\quad (805\text{–}1066\,\mathrm{K}) \tag{4}$$

The simple relation, namely Nernst equation, between the standard Gibbs energy change, $\Delta_r G^\circ$, corresponding to the cell reaction and the cell EMF is given by $\Delta_r G^\circ = -n\mathrm{FE}$. Since EMF is an electrical quantity, that can be measured with high accuracy and precision, the scatter in the experimental data is rather less. For an uncertainty of $\pm 1$ mV and $n = 2$, the corresponding scatter in $\Delta_r G^\circ$ is around 200 J.

from Eq. (9). Even though it appears that the percentage difference between these two values is about 15%, the absolute difference is relatively small. The entropy change, $\Delta_r S^\circ$, is about $-21$ and $-12\,\mathrm{J\,K^{-1}\,mol^{-1}}$ derived from Eqs. (8) and (9) for the solid–solid reaction between equal moles of SrO and $CeO_2$. These values are reasonable owing to the highly disordered structure of $SrCeO_3$. The equilibrium temperature above which SrO, $CeO_2$ and $SrCeO_3$ coexist is given by the Eqs. (8) and (9). These values are 1151 K (for Eq. (8)) and 1247 K (for Eq. (9)). Above this temperature $SrCeO_3$ would decompose into SrO and $CeO_2$.

Gopalan and Virkar [7] measured the EMF of the galvanic cell,

$$CO_2, O_2/SrCO_3 + SrF_2 + Pt|SrF_2|SrCeO_3 + CeO_2 + SrF_2 + Pt/CO_2, O_2 \tag{V}$$

## 4. Discussion

### 4.1. Gibbs energy data on $SrCeO_3$ from Cells (I) and (II)

The two half-cell reactions of cells (I) and (II) are represented by

$$SrO(s) + 2F^- \Rightarrow SrF_2(s) + \frac{1}{2}O_2(g) + 2e^- \tag{5}$$

$$SrF_2(s) + CeO_2(s) + \frac{1}{2}O_2(g) + 2e^- \Rightarrow SrCeO_3(s) + 2F^- \tag{6}$$

The over-all cell reaction (with $n = 2$) could be represented by

$$SrO(s) + CeO_2(s) \Rightarrow SrCeO_3(s) \tag{7}$$

Thus, the standard Gibbs energy change for the reaction (7), $\Delta_r G^\circ$ (7) would directly yield the standard Gibbs energy of formation of one mole of $SrCeO_3$ from the binary oxides SrO and $CeO_2$. In turn, the $\Delta_r G^\circ$ of $SrCeO_3$ was thus derived from Eqs. (1) and (2) to be as follows.

$$\Delta_r G^\circ(SrCeO_3) \pm 0.2(\mathrm{kJ\,mol^{-1}}) = -24.5 + 0.0213T\ (\mathrm{K})\quad (837\text{–}976\,\mathrm{K}) \tag{8}$$

$$\Delta_r G^\circ(SrCeO_3) \pm 0.3(\mathrm{kJ\,mol^{-1}}) = -15.3 + 0.0123T\ (\mathrm{K})\quad (788\text{–}954\,\mathrm{K}) \tag{9}$$

The purpose of assembling galvanic cells with different fluoride electrolytes was to check the consistency of the EMF data. For instance, the $\Delta_r G^\circ$ value at 950 K obtained from Eq. (8) was found to be $-4.3\,\mathrm{kJ\,mol^{-1}}$. This is in very good agreement with $-3.6\,\mathrm{kJ\,mol^{-1}}$ obtained at four temperatures in the range 1223–1373 K. They derived the following expression for the standard Gibbs energy of formation, $\Delta_r G^\circ$ of one mole of $SrCeO_3$ from the constituent binary oxides SrO and $CeO_2$.

$$\Delta_r G^\circ(SrCeO_3)\ (\mathrm{kJ\,mol^{-1}}) = 68.3 - 0.1068T\ (\mathrm{K}) \tag{10}$$

Extrapolation of the expression Eq. (10) to 950 K gives a value of $(\Delta_r G^\circ)$ $-33.1\,\mathrm{kJ\,mol^{-1}}$ which is not in agreement with the values of $-4.3$ and $-3.6\,\mathrm{kJ\,mol^{-1}}$ obtained in the present study. Moreover, the entropy term $\Delta_r S^\circ$ in Eq. (10) is higher than the normally expected values of 6–10 $\mathrm{J\,K^{-1}\,mol^{-1}}$ for a solid–solid reaction. The $(\Delta_r G^\circ)$ values from the cells (I) (Eq. (8)) and (II) (Eq. (9)) are compared with those of the values from cell (V) obtained by Gopalan and Virkar [7] in Fig. 3.

Computation of standard Gibbs energy of formation, $\Delta_f G^\circ$, $SrCeO_3$ from Eq. (7) requires reliable Gibbs energy values for SrO(s) and $CeO_2$(s). Combining the auxiliary data for $\Delta_f G^\circ$ SrO(s) and $CeO_2$(s) obtained from

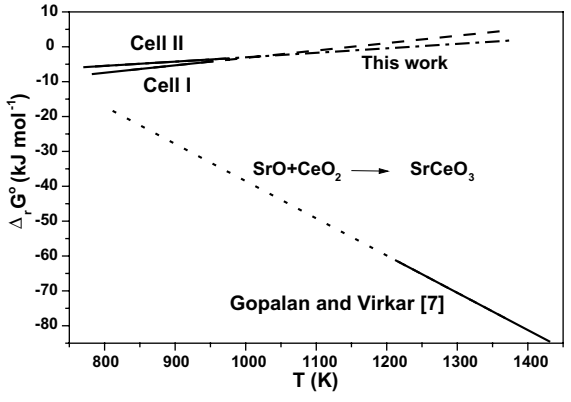


Fig. 3. Comparison of $\Delta_r G^\circ$ of $SrCeO_3$(s) with literature data.

the literature [14] with the values $\Delta_r G^\circ$ ($SrCeO_3$) from Eqs. (8) and (9), the following expressions were derived for the standard Gibbs energy of formation of $SrCeO_3$.

$$\Delta_f G^\circ(SrCeO_3) \pm 14(kJ\,mol^{-1}) = -1706.6 + 0.3379T\ (K) \quad (837\text{–}976\,K) \tag{11}$$

$$\Delta_f G^\circ(SrCeO_3) \pm 14(kJ\,mol^{-1}) = -1697.4 + 0.3289T\ (K) \quad (788\text{–}954\,K) \tag{12}$$

These results indicate that $SrCeO_3$ is only marginally more stable than its constituent oxides.

### 4.2. Gibbs energy data on $SrCeO_3$ from Cell (III)

The fluorine potential over the reference electrode (CaO + $CaF_2$) is higher than that of the test electrode, ($SrCeO_3$ + $CeO_2$ + $SrF_2$) in cell III. The half-cell reactions at the anode and the cathode are given as

$$SrCeO_3(s) + 2F^- \Rightarrow SrF_2(s) + CeO_2(s) + \frac{1}{2}O_2(g) + 2e^- \tag{13}$$

$$CaF_2(s) + \frac{1}{2}O_2(g) + 2e^- \Rightarrow CaO(s) + 2F^- \tag{14}$$

The overall cell reaction (with $n = 2$) is given by

$$CaF_2(s) + SrCeO_3(s) \Rightarrow SrF_2(s) + CeO_2(s) + CaO(s) \tag{15}$$

The standard Gibbs energy change, $\Delta_r G^\circ$ for the above reaction could be calculated from the EMF expression (3) and is given below.

$$\Delta_r G^\circ(15) \pm 0.1\ (kJ\,mol^{-1}) = -29.1 + 0.0059T\ (K) \quad (972\text{–}1142\,K) \tag{16}$$

Combining the above expression along with $\Delta_f G^\circ$ values of $CaF_2$ and $SrF_2$ compiled by Knacke et al. [15] $CeO_2$ by Kubaschewski and Alcock [14] and the assessed values of CaO from the literature [16], the following equation was derived.

$$\Delta_f G^\circ(SrCeO_3) \pm 23(kJ\,mol^{-1}) = -1706.2 + 0.3157T\ (K) \tag{17}$$

The expressions for the $\Delta_f G^\circ$ ($SrCeO_3$) thus obtained from the three cells are compared in Table 5 along with the values obtained by Cordfunke et al. [8] using calorimetric measurements. It could be seen from this table that the individual enthalpy and entropy terms are in excellent agreement among these three cells. At 950 K, the Gibbs energy values from cell I and II are in excellent agreement with each other. Even though the values obtained using cell (III) are in excellent agreement with that reported by Cordfunke et al. [8], these values are marginally more negative. The following average expression obtained from expressions (11), (12) and (17) is recommended for $\Delta_f G^\circ$ ($SrCeO_3$) over the temperature range 788–1142 K.

$$\Delta_f G^\circ(SrCeO_3) \pm 17(kJ\,mol^{-1}) = -1703.4 + 0.3275T\ (K) \tag{18}$$

### 4.3. $\Delta_f H^\circ_{298}$ ($SrCeO_3$) by the third-law method

In order to assess the temperature dependent errors in the EMF measurements of cell (I) and Cell (III) and to verify if these values are consistent with the calorimetric data, it was necessary to carry out the third-law analysis. For this purpose, the values of free energy functions for $SrCeO_3$ in the range 700–1100 K tabulated by Cordfunke et al. [8] were taken. The standard entropy, $S^\circ_{298}$ of $SrCeO_3$ ($131\,J\,K^{-1}\,mol^{-1}$) was used for the calculation of the Gibbs energy function of $SrCeO_3$. These values of the Gibbs energy functions were then combined with the corresponding values for the elements, viz., Sr(s) from Ref. [17], Ce(s), and $O_2$(g) from Ref. [18] in order to derive the Gibbs energy function for $SrCeO_3$. The values thus obtained were combined with the values of $\Delta_r G^\circ$ calculated from each EMF value (Table 1) along with $\Delta_f G^\circ$ of SrO and $CeO_2$ from the literature to derive

Table 5
Comparison of $\Delta_f G^\circ$ ($SrCeO_3$) values obtained from different cells along with the $\Delta_f H^\circ_{298}$ values from the literature

| Galvanic cells | $\Delta_f G^\circ$ (kJ mol$^{-1}$) = $A + B \cdot T$ (K) | | $T$ range (K) | $\Delta_f G^\circ$ (950 K) (kJ mol$^{-1}$) | $\Delta_f H^\circ_{298}$ (kJ mol$^{-1}$) | Reference |
|---|---|---|---|---|---|---|
| | $A$ | $B$ | | | | |
| Cell I | −1706.6 | 0.3379 | 837–976 | −1385.5 | −1675.3 ± 10.8 | This work |
| Cell II | −1697.4 | 0.3289 | 788–954 | −1385.0 | – | This work |
| Cell III | −1706.2 | 0.3157 | 972–1142 | −1406.3 | −1676.3 ± 12.8 | This work |
| Average | −1703.4 | 0.3275 | 788–1142 | −1392.2 | | This work |
| | | | | −1405.6 | −1687 ± 2.7 | [8] |
| | | | | | −1737 ± 22 | [7] |
| | | | | | −1685.6 ± 3.8 | [19] |

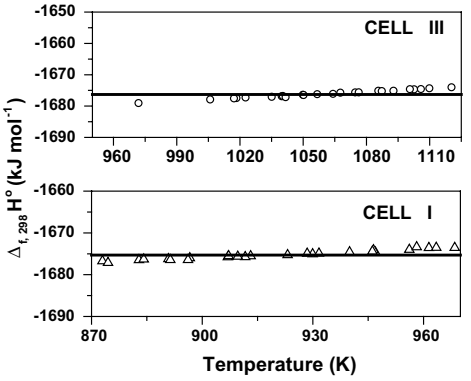


Fig. 4. Third-law treatment of the standard enthalpy of formation of $SrCeO_3$(s) at 298.15 K, from cells I and III.

$\Delta_f H^\circ_{298}$ of $SrCeO_3$. Similar exercise was done for cell (III) using $\Delta_f G^\circ$ of CaO, $CaF_2$ and $SrF_2$ from the literature to derive $\Delta_f H^\circ_{298}$ of $SrCeO_3$ at different experimental temperatures.

The third-law plots of $\Delta_f H^\circ_{298}$ of $SrCeO_3$ derived from cells (I) and (III) are shown in Fig. 4. The mean value was found to be $-(1675.3 \pm 10.8)\,kJ\,mol^{-1}$ from cell (I) and $-(1676.3 \pm 12.8)\,kJ\,mol^{-1}$ from cell (III). The values of $\Delta_f H^\circ_{298}$ show a weak dependence on temperature. In view of the small magnitude of this dependence (about $0.04\,kJ\,mol^{-1}$) it is reasonable to assume that these temperature dependent errors will be well within the random errors in the measured values. These are found to be in fair agreement with the values viz., $-(1687 \pm 2.7)$ and $-(1685.6 \pm 3.8)$ $kJ\,mol^{-1}$ reported by Cordfunke et al. [8] and Goudiakas et al. [19], respectively. These values are compared in Table 5 as well. However, the data obtained using the cell (II) were not analyzed using the third-law method, for it appeared to have significant temperature dependent errors.

### 4.4. Thermodynamic stability of $Sr_2CeO_4$

The EMF results from cell (IV) represented by Eq. (4), over the temperature range 805–1066 K are given in Table 4. The half-cell reactions are given as

$$SrO(s) + 2F^- \Rightarrow SrF_2(s) + \frac{1}{2}O_2(g) + 2e^- \quad (19)$$

$$SrF_2(s) + SrCeO_3(s) + \frac{1}{2}O_2(g) + 2e^- \Rightarrow Sr_2CeO_4(s) + 2F^- \quad (20)$$

The overall cell reaction (with $n = 2$) could be represented by

$$SrCeO_3(s) + SrO(s) \Rightarrow Sr_2CeO_4(s) \quad (21)$$

The standard Gibbs energy change, $\Delta_r G^\circ$ for the above reaction (21) calculated using the expression (4) is given below:

$$\Delta_r G^\circ(21) \pm 0.2(kJ\,mol^{-1}) = -11.62 + 0.01057T\ (K) \quad (22)$$

An expression for $\Delta_f G^\circ$ of $Sr_2CeO_4$ was derived by combining the expressions (18), (22) and (21) along with the values for $\Delta_f G^\circ$ (SrO) obtained from the literature [14].

$$\Delta_f G^\circ(Sr_2CeO_4) \pm 21(kJ\,mol^{-1}) = -2307.1 + 0.4400T\ (K) \quad (805–1066\,K) \quad (23)$$

An expression for the standard Gibbs energy of formation of $Sr_2CeO_4$ is reported in this study for the first time. A third-law analysis of the EMF results could not be carried out owing to the lack of Gibbs energy functions on $Sr_2CeO_4$. However, Ali et al. [10] have measured $\Delta_f H^\circ_{298}$ of $Sr_2CeO_4$ by solution calorimetry. This value is found to be $-2280\,kJ\,mol^{-1}$ and is in good agreement with the second-law enthalpy value of $-2307\,kJ\,mol^{-1}$ at the mean experimental temperature of 936 K, obtained in the present study.

## 5. Conclusion

The standard Gibbs energy of reaction, $\Delta_r G^\circ$ from cells (I) and (II) reveals that $SrCeO_3$(s) is only marginally stable with respect to its constituent binary oxides in the temperature range amenable to fluoride electrolyte measurements. The $\Delta_f G^\circ$ ($SrCeO_3$(s)) values determined from three different cells using different fluoride electrolytes as well as different reference electrodes match reasonably well. In addition, the standard Gibbs energy of formation, $\Delta_f G^\circ$ ($Sr_2CeO_4$) was also determined for the first time by the fluoride EMF technique.

## References

[1] V. Venugopal, Indian Assoc. Nucl. Chem. Allied Sci. (IANCAS) Bull. I (4) (2002) 19.
[2] H.S. Kamath, A. Kumar, Indian Assoc. Nucl. Chem. Allied Sci. (IANCAS) Bull. I (4) (2002) 26.
[3] H. Kleykamp, J. Nucl. Mater. 131 (1985) 221.
[4] M.A. Mignanelli, P.E. Potter, J. Nucl. Mater. 118 (1983) 150.
[5] JCPDS, International Centre for Diffraction Data, file Nos. 22-1422, 23-1412, 1999.
[6] R. Saha, R. Babu, K. Nagarajan, C.K. Mathews, J. Nucl. Mater. 167 (1989) 271.
[7] S. Gopalan, V. Virkar, J. Electrochem. Soc. 140 (1993) 1060.
[8] E.H.P. Cordfunke, A.S. Booij, M.E. Huntelaar, J. Chem. Thermodyn. 30 (1998) 437.

[9] S. Yamanaka, K. Kurosaki, T. Matsuda, S. Kobayashi, J. Alloys Compd. 352 (2003) 52.
[10] M. Ali, S.R. Bharadwaj, D. Das, in: Proceedings of the 14th National Symposium on Thermal Analysis (THERMANS 2004), M.S. University, Baroda, India, 2004, p. 162.
[11] K. Ananthasivan, S. Anthonysamy, C. Sudha, A.L.E. Terrance, P.R. Vasudeva Rao, J. Nucl. Mater. 300 (2002) 217.
[12] A.M. Azad, O.M. Sreedharan, J. Appl. Electrochem. 17 (1987) 949.
[13] A.M. Azad, R. Sudha, O.M. Sreedharan, Thermochim. Acta 194 (1992) 129.
[14] O. Kubaschewski, C.B. Alcock, Metallurgical Thermochemistry, 5th Ed., Pergamon, Oxford, 1983.
[15] O. Knacke, O. Kubaschewski, K. Hesselmann (Eds.), Thermochemical Properties of Inorganic Substances, 2nd Ed., Springer-Verlag, Germany, 1991.
[16] O.M. Sreedharan, C. Mallika, A Compilation of Gibbs Energy Data for 40 Metal Oxide Buffers, Report RRC – 69, 1984.
[17] M.W. Chase, Jr., C.A. Davis, J. Downey, Jr., D.J. Frurip, R.A. McDonald, A.N. Syveud, JANAF Thermochemical Tables, 3rd Ed., 1985.
[18] R. Hultgren, P.D. Desai, D.T. Hawkins, M. Gleiser, K.K. Kelley, D.D. Wagman, Selected Values of the Thermodynamic Properties of Elements, American Society for Metals, Metals Park, Ohio, 1973.
[19] J. Goudiakas, R.G. Haire, J. Fuger, J. Chem. Thermodyn. 22 (1990) 577.